Hydrogen atom lifetimes in the three-dimensional heliosphere over the solar cycle

Wayne R. Pryor,[1] Joseph M. Ajello,[2] David J. McComas,[3] Manfred Witte,[4] and W. Kent Tobiska[5]

Received 31 January 2003; revised 19 May 2003; accepted 3 June 2003; published 15 August 2003.

[1] The three-dimensional (3-D) structure of the heliosphere is investigated using in situ and remote sensing measurements. The 3-D structure of both neutral interplanetary gas and solar wind ions are affected by the solar latitude variation of the solar radiation fields (solar wind and solar EUV). Neutral hydrogen atom lifetimes against charge-exchange with solar wind protons in the 3-D heliosphere are calculated from measurements of the solar wind proton velocity, density, and mass flux by Ulysses SWOOPS (Solar Wind Observations Over the Poles of the Sun) from 1990–2001. These are compared to in-ecliptic H atom lifetimes derived from solar wind measurements by the spacecraft IMP (Interplanetary Monitoring Platform) 6, 7, and 8, WIND, and ACE (Advanced Composition Explorer) SWEPAM (Solar Wind Electron Proton Alpha Monitor). Recent observations during the Ulysses rapid solar pole-to-solar pole passage (fast-latitude scan) at solar maximum find a more isotropic rotationally averaged solar wind mass flux (and H atom lifetime) than was found during the previous fast latitude scan at solar minimum. During the solar minimum fast-latitude scan the 27-day averaged SWOOPS lifetime passed through two distinct regimes: it doubled from 2×10^6 s at low latitudes to 4×10^6 s at high latitudes in both hemispheres. During the solar maximum pass the 27-day averaged SWOOPS H atom lifetime (corrected to 1 AU) at all southern latitudes and at all northern latitudes below 60° was $(2-2.5) \times 10^6$ s, while at the very end of the pass, above 60° N latitude, it rose to 4×10^6 s as polar coronal holes reformed. Remote sensing studies of interplanetary H Lyman-α emission, white light solar coronal observations, and radio scintillation experiments have also indicated that the time-averaged solar wind mass flux (and H atom lifetime) is more isotropic at solar maximum than at solar minimum. This enlarges the polar H cavity at solar maximum. Results from in situ measurements are compared to remote sensing data. Ulysses GAS Lyman-α maps are modeled, with updated results. Comparisons of the H atom charge exchange loss rate with a weaker H atom loss process, photoionization, are made using the SOLAR2000 model [*Tobiska et al.*, 2000] for in-ecliptic solar Extreme UltraViolet (EUV) fluxes. The relative latitude invariance of the H atom lifetime at solar maximum is related to the absence of high-speed solar wind at solar maximum and to the large inclination of the heliospheric current sheet. *INDEX TERMS:* 2151 Interplanetary Physics: Neutral particles; 2144 Interplanetary Physics: Interstellar gas; 2164 Interplanetary Physics: Solar wind plasma; 2162 Interplanetary Physics: Solar cycle variations (7536); *KEYWORDS:* interplanetary hydrogen, solar wind, interstellar wind, charge-exchange, Ulysses

Citation: Pryor, W. R., J. M. Ajello, D. J. McComas, M. Witte, and W. K. Tobiska, Hydrogen atom lifetimes in the three-dimensional heliosphere over the solar cycle, *J. Geophys. Res.*, *108*(A10), 8034, doi:10.1029/2003JA009878, 2003.

1. Introduction

[2] The ESA/NASA Ulysses Mission has now explored the solar poles and solar equator during both solar minimum and solar maximum, providing a unique opportunity to look for systematic changes in solar wind properties. Details of the solar wind properties found with Ulysses SWOOPS have been presented elsewhere [*McComas et al.*, 2000a, 2000b, 2001, 2002a, 2002b; *McComas*, 2002]. Here we report on the Ulysses solar wind mass flux at both solar maximum and solar minimum and draw conclusions about

[1]Center for Atmospheric Sciences, Hampton University, Hampton, Virginia, USA.
[2]Jet Propulsion Laboratory, Pasadena, California, USA.
[3]Southwest Research Institute, San Antonio, Texas, USA.
[4]Max-Planck Institut fur Aeronomie, Katlenburg-Lindau, Germany.
[5]Space Environment Technologies SpaceWx Division, Los Angeles, California, USA.

0148-0227/03/2003JA009878$09.00

the lifetime of heliospheric H atoms. *McComas et al.* [1999] reported on H atom lifetimes from the first solar minimum orbit (up to December 1997) and found that H atoms survived longer at high solar latitudes than near the ecliptic plane. H atom lifetimes are of interest for studies of comets, the geocorona, planetary exospheres, and the heliosphere. Heliospheric H Lyman-α emissions are sensitive to the H atom lifetime, providing a way of remotely sensing the solar wind mass flux, a technique that will be discussed and evaluated here using in situ solar wind measurements from Ulysses and other spacecraft.

[3] Neutral atoms such as H and He in the solar system primarily come from interstellar space, approaching the sun from the "upwind" direction. Neutral helium measurements by the Ulysses GAS experiment find that the upwind flow comes from 254.7 ± 0.5 ecliptic longitude, 5.2 ± 0.2 ecliptic latitude [*Witte et al.*, 2003] with a velocity of 26.3 ± 0.4 km/s and a gas temperature of 6300 ± 340 K at large distances from the sun. For H, recent measurements by SOHO SWAN indicate a somewhat lower velocity ~21–23 km/s and a higher temperature ~10,000–13,000 K [*Costa et al.*, 1999], with the difference between H and He properties attributed to outer heliospheric H-H+ charge exchange [e.g., *Izmodenov et al.*, 1999].

[4] Charge exchange within a few AU from the Sun between solar wind protons traveling at 400–700 km/s and slow heliospheric H atoms produces fast neutral H atoms and H^+ pick-up ions traveling radially away from the Sun, leaving a cavity near the Sun depleted in slow neutral H that can effectively scatter the solar Lyman-α line and produce the observed Lyman-α background glow [e.g., *Thomas*, 1978]. (Solar EUV photoionization also removes neutral H near the Sun at a slower rate). The shape of the hydrogen cavity depends, among other things, on the latitude dependence of the solar wind mass flux, or more precisely, on the latitude dependence of the product of the time-averaged proton density, velocity, and the velocity-dependent cross section. A number of studies of the Lyman-α glow have attempted to infer the solar wind mass flux variation with latitude, with different results at different times. We show below that the varying results inferred from Lyman-α measurements during the period from 1990–2001 are as expected, based on the changing solar wind measurements from Ulysses SWOOPS.

2. Ulysses SWOOPS Measurements of the H Lifetime

[5] Ulysses SWOOPS [*Bame et al.*, 1992] measurements on solar wind ions and electrons have been obtained since 17 November 1990 following launch on the space shuttle Discovery on 6 October 1990. The Ulysses trajectory remained near the ecliptic plane until the Jupiter swingby gravitationally altered the trajectory in February 1992. The spacecraft then traveled south from the ecliptic, traversing the Sun's south polar region in September 1994. A rapid pole-to-pole scan ("fast latitude scan") at solar minimum (September 1994–July 1995) was then followed by slow descent from the north pole, an ecliptic plane crossing near 5 AU in April 1998, and the recent fast-latitude scan at solar maximum from over the south polar region in November 2000 to the north polar region in October 2001.

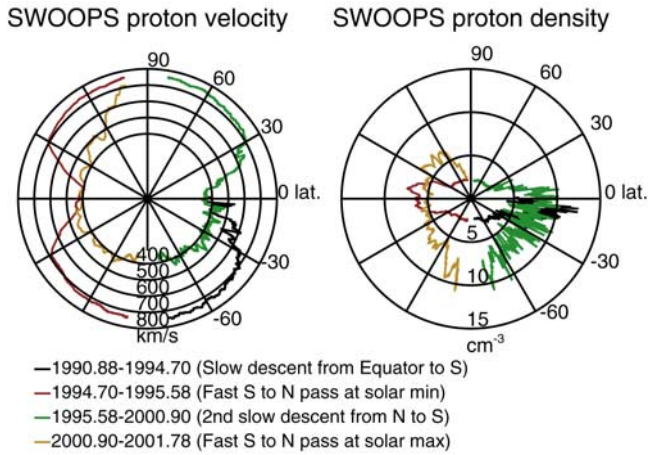

Figure 1. Polar plots of the Ulysses SWOOPS solar wind proton velocity in km/s and solar wind proton density measurements in cm^{-3} (scaled to 1 AU, assuming a $1/d^2$ fall-off with heliocentric distance d). Latitudes in all figures are heliographic.

[6] Figure 1 shows the 27-day averaged (solar-rotation averaged) solar wind proton velocity (v_p) and density (n_p) measurements from Ulysses SWOOPS. (Whenever an average is mentioned in this paper, it refers to the average of the values over the specified time interval, centered on the time in question. An alternative choice, averaging over the time preceding the measurement, skews the results in latitude as Ulysses orbits the Sun). This 27-day averaging process removes a great deal of structure due to persistent longitudinal asymmetries in the solar wind, making it easier to see the long-term trends important for understanding the H distribution. The SWOOPS pre-launch instrument calibration determines velocity to better than 1% and density, at least at the time of the calibration, to about 10%. *Joselyn and Holzer* [1974] proposed that Lyman-α remote sensing observations of the cavity shape could be used to remotely infer a quantity closely related to the latitude dependence of the solar wind mass flux $n_p v_p$, that is, the H-H^+ solar wind charge exchange rate R_{sw}.

$$R_{sw} = n_p\, v_p \sigma(v_p), \tag{1}$$

where n_p is the solar wind proton density, v_p is the solar wind proton velocity, and $\sigma(v_p)$ is the velocity-dependent charge-exchange cross section. Cross section values we have adopted from *Barnett* [1990] decline from $1.83 \times 10^{-15}\,cm^2$ at $350\,km\,s^{-1}$ (slow solar wind) to $1.24 \times 10^{-15}\,cm^2$ at 750 km s^{-1} (fast solar wind). Figure 2 show the SWOOPS-derived H atom lifetimes against charge-exchange ($\tau_{sw} = 1/R_{sw}$) and charge-exchange rates R_{sw}, using equation (1). To obtain Figure 2, R_{sw} was computed for each measurement and averaged over 27 days to obtain a rotationally averaged charge-exchange rate, the inverse of which is the average lifetime. Note that directly averaging the lifetime from $1/R_{sw}$ leads to incorrect average lifetimes. Averaging is desirable for studying the Lyman-α, since the H density reflects conditions over a year or more before the observations (an H atom travels 4.2 AU/year at 20 km/s). Averaging for longer than 27 days oversmooths the data

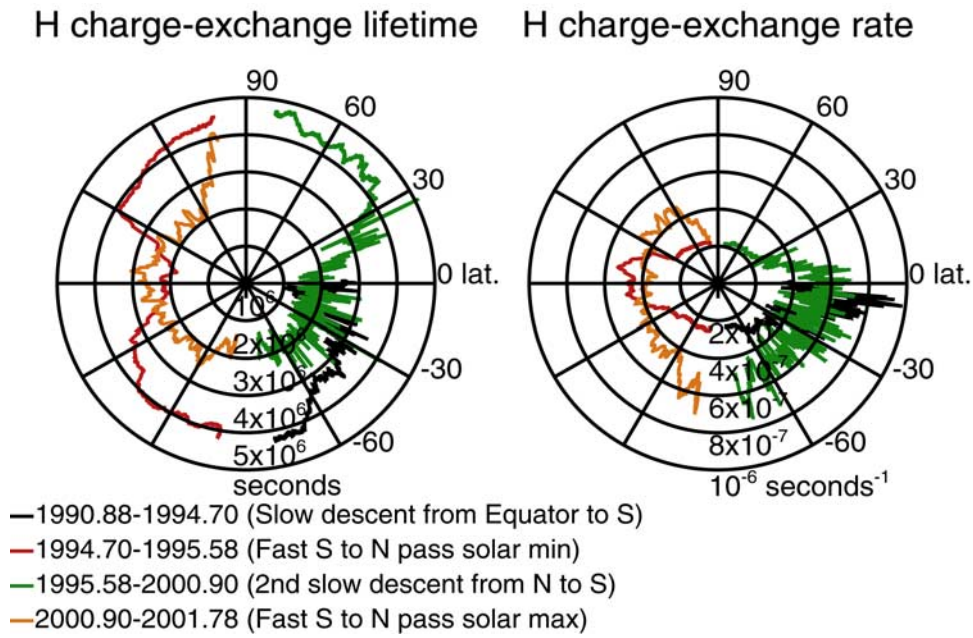

Figure 2. Polar plot of the 27-day averaged Ulysses SWOOPS H atom lifetimes against charge-exchange in s and charge-exchange rates in s^{-1} at 1 AU. A 27-day lifetime (almost 1 month) would correspond to 27 days times 86,400 s/day = 2.3×10^6 s. Note that charge-exchange rates were somewhat more isotropic during the current solar maximum fast-latitude scan than during the previous solar minimum fast-latitude scan.

from the fast latitude scans when the latitude of Ulysses was changing rapidly, removing real observed structure as a function of latitude. Figure 2 also shows the charge exchange rates themselves, which are perhaps easier to understand than lifetimes, since a large solar wind mass flux directly leads to a large charge-exchange rate.

[7] Examination of the SWOOPS results in Figure 2 leads to the conclusion that in 1998–2001 the H atom lifetime against charge-exchange was generally latitude invariant, with a 27-day average value at 1 AU of $(2.0\ (+1.0,-0.5)) \times 10^6$ s. An exception to this pattern is an increase in the lifetime to 4×10^6 s at the very highest northern heliographic latitudes above 60°, due to the reappearance of high latitude coronal holes in this period [*McComas et al.*, 2002a, 2002b]. This is quite different from the solar minimum data that contain high speed solar wind at high latitudes and a corresponding increase in 27-day average H atom lifetime from $(2.0\ (+1.0, -0.5)) \times 10^6$ s near the ecliptic to $(4.0 \pm 0.5) \times 10^6$ at high heliographic latitudes. At low heliographic latitudes the measured 27-day average H atom lifetimes remain near $(2.0\ (+1.0, -0.5)) \times 10^6$ s at both solar minimum and solar maximum. Some caution is needed in interpreting the in situ data to derive lifetimes at all latitudes and times, because the solar wind was changing while the spacecraft was moving. Remote sensing measurements remain important for identifying the rapidly changing boundaries between the fast and slow solar wind regions.

3. Comparisons With In-Ecliptic Measurements

[8] In situ measurements from a single spacecraft are inadequate to describe changes in a complex structure like the 3-D heliosphere. However, substantial progress can be made by comparing measurements from low heliographic latitude solar wind monitoring spacecraft in the vicinity of Earth with the Ulysses measurements from a variety of heliographic latitudes.

[9] We obtained solar wind data for the in-ecliptic study from two sources: the National Space Science Data Center (NSSDC) OMNIWEB solar wind plasma database (available at http://nssdc.gsfc.nasa.gov) and the ACE SWEPAM web site (available at http://swepam.lanl.gov/text.html). The OMNIWEB data we examined, from 1973-2001 represent merged solar wind measurements from NASA's IMP 6, 7, 8, and WIND spacecraft and are currently available for most days in this period. IMP 6 was launched on 13 March 1971 and reentered Earth's atmosphere on 2 October 1974. IMP 7 was launched on 23 September 1972 and turned off on 31 October 1978. Data from IMP 8 were available after its launch on 26 October 1973. These data sets are extensively described by *King* [1977, 1979, 1989], *Couzens and King* [1986], and *King and Papitashvili* [1994]. The most recent solar wind plasma data merged in OMNIWEB comes from the WIND Solar Wind Experiment [*Ogilvie et al.*, 1995], launched on 1 November 1994. The ACE SWEPAM [*McComas et al.*, 1998] data are the newest, and represent only a few years of data, beginning after the launch on 25 August 1997. They have not yet been merged into OMNIWEB but are shown here to complete the comparisons. OMNIWEB has substantial overlap in time with the Ulysses data that began in 1990.

[10] Figure 3 brings together several related kinds of time-series data from 1973 to 2001, the time of Ulysses' most recent polar passage. The top panel shows the solar F10.7 cm radio flux, a commonly used solar activity indicator available at www.spacewx.com. The middle panel shows the heliographic latitudes of Ulysses and the Earth. The third panel compares various measures of the H loss

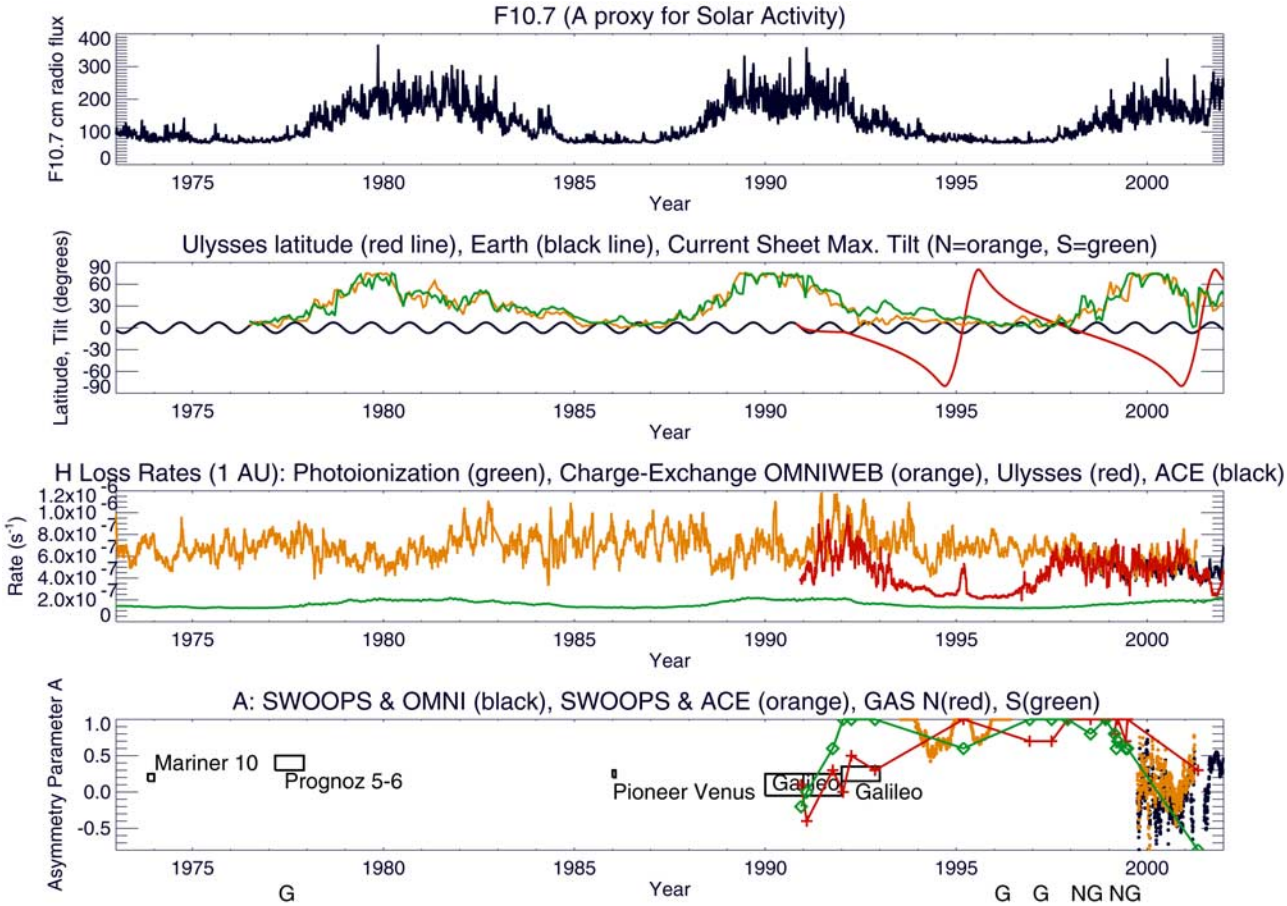

Figure 3. (top panel) The solar F10.7 cm radio flux is shown as a function of time. (second panel) The heliographic latitudes of the Ulysses spacecraft and the Earth are displayed as a function of time. Also shown is the maximum extent of the heliospheric current sheet tilt in each hemisphere away from the ecliptic [*Hoeksema et al.*, 1982, 1983; *Hoeksema*, 1991] where the actual data used here is from the radial field model data given at the web site http://sun.stanford.edu/∼wso/Tilts.html. (third panel) Loss processes for H, including a 27-day average photoionization estimate, 27-day average charge exchange measurements from the OMNI data, 27-day average charge exchange measurements from the ACE SWEPAM data, and 27-day average charge exchange measurements from Ulysses SWOOPS. (bottom panel) The solar wind asymmetry parameter is shown as a function of time. Boxes represent reported asymmetry values derived from Lyman-α measurements by Mariner 10, Prognoz 5-6, Pioneer Venus, and Galileo, with the box width set by the duration of the observation, and the box height set by the reported error bars. Ulysses GAS Lyman-α values show the derived asymmetry parameter in the north and south separately. Years when a heliospheric upwind groove was or was not reported are marked with a "G" or an "NG." The first "G" is from Prognoz [*Bertaux et al.*, 1985, 2003], the next two G's for 1996 and 1997 are from SOHO SWAN [*Bertaux et al.*, 1997, 1999], and the two NG's for 1998 and 1999 are also from SOHO SWAN [*Summanen et al.*, 2002]. Also shown are estimates for A found by comparing loss rates found by Ulysses and near-Earth spacecraft.

rate, and the bottom panel shows various estimates of the H atom lifetime asymmetry parameter, A, to be explained later.

[11] A secondary H loss process shown in Figure 3 is the solar EUV photoionization rate, based on the SOLAR2000 model of the solar spectrum and its variations in time [*Tobiska et al.*, 2000], available at www.spacewx.com. Nearly all space-based measurements of the solar extreme ultraviolet irradiances since the mid-1970s have been incorporated into the derivation of SOLAR2000 including 13 rockets, one reference spectrum, one theoretical spectrum, and time-series measurements from 21 instruments on five spacecraft. The SOLAR2000 model provided solar fluxes that were combined with the well-known H photoionization cross-sections tabulated by *Banks and Kockarts* [1973] to find EUV photoionization rates. The result is better illustrated in Figure 4, where this photoionization rate estimate is compared to the curve we had been using in earlier modeling efforts [e.g., *Pryor et al.*, 1998a, 1998b, 2001]. That curve was based on work by *Ogawa et al.* [1995], specifically their Table 3 specifying loss rates at solar maximum and minimum. EUV uncertainties remain large, and we have not attempted to calculate here the latitude dependence of the photoionization. This will depend on the

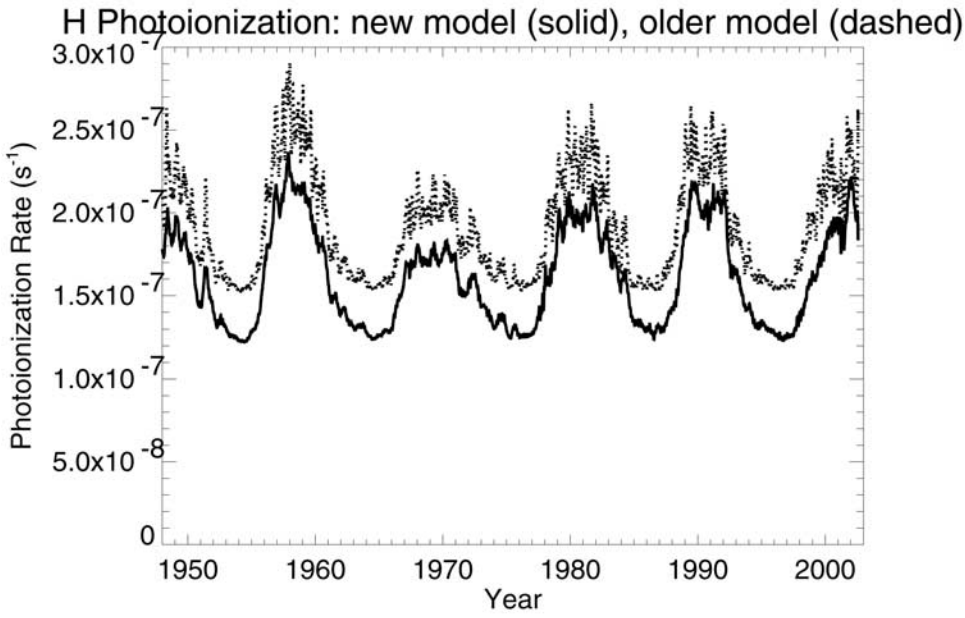

Figure 4. Detailed comparison of the estimated H atom photoionization rate at 1 AU as a function of time using the *Tobiska et al.* [2000] SOLAR2000 model with an earlier estimate that we had been using based on Table 3 of *Ogawa et al.* [1995].

latitude and longitude distribution of EUV bright active regions and the limb darkening and/or brightening behavior at each wavelength in the photoionization continuum below 91.2 nm. Ulysses GAS data indicate that there is a substantial latitude dependence of the He photoionization rate at solar maximum [*Witte et al.*, 2003]. We have neglected weaker H loss processes, such as electron impact ionization [e.g., *Rucinski et al.*, 1996] and long-wavelength photoionization of metastable H excited by solar Lyman-β [*Gruntman*, 1990; *Ogawa et al.*, 1995].

[12] The primary H atom loss-process is the charge-exchange process. The third panel of Figure 3 shows the 27-day averages of the charge-exchange rate for the OMNIWEB IMP 6, 7, and 8 and WIND data. Also shown are 27-day averages of the charge-exchange rate for the ACE data, which shows good agreement with the OMNIWEB data in the overlap region. The same panel also shows the 27-day average Ulysses SWOOPS charge-exchange rates obtained at a variety of latitudes. We have assumed the nominal calibrations for each solar wind instrument. (*Bzowski* [2001a] investigated correction factors that might be needed to bring the various solar wind data sets into better agreement). The comparison we have found between the Ulysses and the other solar wind measurements is very different during the solar minimum and solar maximum periods.

[13] During the solar minimum fast-latitude scan of Ulysses in 1994–1995 the charge exchange rate at high latitudes was much lower than the in-ecliptic measurements by Ulysses and IMP. This was during a period of low heliospheric current sheet tilt (see the middle panel) when dense slow solar wind was found near the ecliptic, causing a large charge-exchange rate, while less dense, high-speed solar wind was found at high latitudes.

[14] During the recent solar maximum fast-latitude scan of Ulysses in 2000–2001 the charge exchange rate is quite similar in the measurements by ACE, IMP, and Ulysses, even when Ulysses is at high solar latitudes. The curves converge in the plots from about 1998 on. This more isotropic solar wind charge-exchange rate is associated with a period of little or no high-speed solar wind and high current sheet tilt so that dense, slow solar wind associated with the current sheet can be found at a variety of latitudes.

4. Lyman-α Studies of the Solar Wind

[15] We will now compare the in situ results reported above with inferences from many years of Lyman-α remote sensing. Interplanetary Lyman-α is a bright ($\sim$1 kRayleigh) emission easy to study with ultraviolet telescopes in space. An early study [*Thomas and Krassa*, 1971] of Orbiting Geophysical Observatory (OGO) 5 Lyman-α data found an upwind brightness maximum was present during solar maximum. One use of the Lyman-α data in numerous subsequent studies has been to try to estimate the latitude behavior of the solar wind mass flux. Because of the fall-off in H-H^+ charge exchange cross-section with velocity, high-speed solar wind is relatively less effective at producing charge exchange than low-speed solar wind with the same mass flux $n_p v_p$. Also, high-speed solar wind is generally of lower density than low-speed solar wind. These two effects lead to the expectation that heliospheric latitudes dominated by the high-speed solar wind, originating in coronal holes that are most frequently found at high heliographic latitudes near solar minimum, will have relatively more slow H atoms and be brighter in a Lyman-α map. This expectation was tested in heliospheric Lyman-α maps obtained by the Mariner 10 Ultraviolet Spectrometer (UVS) on 6 November 1973–28 January 1974 during solar minimum [*Broadfoot and Kumar*, 1978; *Kumar and Broadfoot*, 1978, 1979; *Ajello*, 1978; *Ajello et al.*, 1979; *Witt et al.*, 1979, 1981]. Brightness maxima at high latitudes were found to be

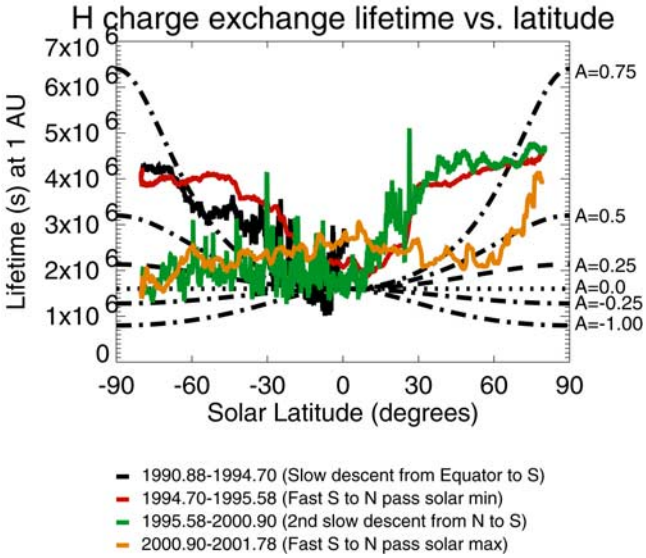

Figure 5. The "asymmetry parameters" used most frequently by Lyman alpha modelers to describe the latitude dependence of the H atom lifetime against charge exchange are illustrated for cases A = −1.0, 0, −0.25, 0.25, 0.5, and 0.75. Also shown are the measured 27-day averaged lifetimes against charge exchange as a function of latitude for the Ulysses SWOOPS experiment.

consistent with an H atom lifetime against charge-exchange $\tau_{sw} = 1/R_{sw}$ of the functional form

$$\tau_{sw}(\text{latitude}) = \tau_{sw}(\text{equator})/\left(1 - \text{A}\ \sin^2\ \text{latitude}\right) \qquad (2)$$

If A = 0, the lifetime is latitude invariant. If A = 0.5, the H atom lifetime against charge-exchange at the pole is twice the lifetime at the equator. Figure 5 illustrates the functional form of τ for several values of A. Models of the Mariner 10 UVS data indicated A = 0.25 ± 0.1. Pioneer Venus Orbiter UVS [*Stewart*, 1980] observations during a special Comet Halley observing sequence from 1 January–4 March 1986 (solar minimum) that covered a range of heliospheric latitudes also found an enhanced H atom lifetime at high latitudes, with a derived A value of A = 0.3 ± 0.2 [*Ajello*, 1990] or A = 0.3 ± 0.05 [*Lallement and Stewart*, 1990]. (Most Pioneer Venus Orbiter UVS measurements were obtained at a constant latitude of −30 degrees and are less suitable for assessing the A parameter that measures latitudinal variations in lifetime. *Lallement et al.* [1990] report that Voyager Lyman-α maps are also relatively insensitive to A because the two Voyager spacecraft were flying upwind and spent most of their time outside the H cavity near the Sun).

[16] Prognoz satellite Lyman-α data from 1977 [*Bertaux et al.*, 1996] found that not only was the H lifetime enhanced at the poles, but also a well-defined "groove" of reduced emission was present in the Lyman-α pattern near the upwind ecliptic plane. This groove can be associated with a period of small heliospheric current sheet tilt [*Hoeksema et al.*, 1982, 1983, 1991] during this period (Figure 3). Enhanced slow solar wind flux near the current sheet depletes the slow neutral H population near the ecliptic plane, leading to the observed groove.

[17] A rather different situation was inferred from 1990–1992 solar maximum Lyman-α data obtained by the Galileo Ultraviolet Spectrometer and Extreme Ultraviolet Spectrometer [*Hord et al.*, 1992; *Pryor et al.*, 1992, 1996, 2001; *Ajello et al.*, 1993, 1994]. Those authors found a brightness maximum in the upwind ecliptic plane and modeled this with a combination of enhanced solar flux from Lyman-α active regions near the ecliptic plane and a nearly isotropic solar wind mass flux. The isotropic solar wind mass flux was considered plausible based on white light images of the Sun which showed a more isotropic and chaotic illumination pattern associated with the large heliospheric current sheet tilt at solar maximum, not the well-defined white-light brightness maximum in the ecliptic plane seen near solar minimum. Galileo UVS "antisun" maps of the downwind hemisphere obtained in 1990 were best fit [*Pryor et al.*, 2001] with A = 0.0, while a map obtained in 1992 required a larger asymmetry factor of A = 0.25. Galileo EUVS data obtained on great circles through the ecliptic poles from this period also can be described with A = 0 in 1990 increasing to A = 0.25 in 1992.

[18] Lyman-α observations by the Ulysses GAS experiment [*Witte et al.*, 1992, 1996] from 1990–1995 were used to infer that the solar wind asymmetry increased over this period from A = 0 to values of A > 0.5 [*Pryor et al.*, 1998b]. Better fits to these data were obtained using other functional forms of the lifetime based on actual SWOOPS measurements. Ulysses GAS upwind measurements from 1997 were well represented using the functional form given by *McComas et al.* [1999] and *Pryor et al.* [2001]. The model charge exchange rate R (s^{-1}) at 1 AU as a function of heliographic latitude θ in radians is

$$R(\theta) = 2.45 \times 10^{-7} + 3.95 \times 10^{-7} e^{-6.37\sin^2\theta}\ s^{-1} \qquad (3)$$

based on SWOOPS data from when Ulysses was 2.0–5.4 AU from the Sun. The period of increasing A value corresponds to a period of declining heliospheric current sheet tilt. *Bzowski et al.* [2002] examined alternate expressions for the ionization profile.

[19] The Solar Heliospheric Observatory (SOHO) SWAN (Solar Wind Anisotropy Experiment) is a dedicated heliospheric Lyman-α instrument that has produced frequent all-sky Lyman-α maps beginning in December 1995 [*Bertaux et al.*, 1995, 1997, 1999]. These maps initially confirmed the Prognoz detection of an upwind ecliptic minimum "groove" during a period of small heliospheric current sheet tilt. *Kyrola et al.* [1998] modeled the 1996 SWAN data, including separate north and south anisotropy (A) parameters and found the A parameters were small (−0.1 to 0.2) outside of a narrow (11.5 degree) enhanced ionization belt near the current sheet. Later reports from SWAN indicate that the groove had weakened [*Bertaux et al.*, 1999] and then was finally replaced by an upwind maximum in 1998 and 1999 [*Summanen et al.*, 2002]. Figure 3 illustrates that these changes correspond to a period of increasing heliospheric current sheet tilt and to a period when the equatorial charge exchange rates converge with the high-latitude charge exchange rates measured by Ulysses. The enhanced solar wind flux produced near the current sheet is now spread over more latitudes, weakening and finally eliminating the groove. *Pryor et al.* [2001] found a Lyman-α plateau or

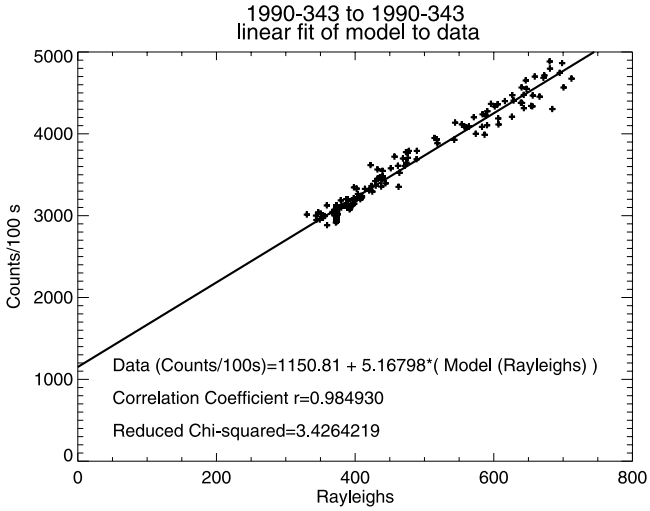

Figure 6. The least-squares fit between Ulysses GAS Lyman-α data and the best of 441 models is illustrated. In this case the linear correlation coefficient was r = 0.98.

weak groove in Ulysses GAS observations of the upwind direction during the period from 1997-336 to 1997-354, rather than the strong maximum seen in Galileo data from the previous solar maximum. This is in general agreement with SOHO SWAN observations from this period [*Bertaux et al.*, 1999]. (We note that Figure 4 of *Pryor et al.* [2001] contains a labeling error: the middle panel should read model, not data). Figure 3 of the current paper illustrates that these changes in the SWAN and GAS data correspond to a period of increasing heliospheric current sheet tilt and to a period when the equatorial charge exchange rates converge with the high-latitude charge exchange rates measured by Ulysses. The enhanced solar wind flux produced near the current sheet is now spread over more latitudes, weakening and finally eliminating the groove.

[20] Figure 5 illustrated one way to estimate A from the Ulysses data alone. This technique may confuse spatial and temporal variations, as the Ulysses spacecraft takes months to years to survey a range of latitudes. Alternatively, the existence of simultaneous H atom lifetime measurements in the ecliptic plane from IMP-8, WIND, and ACE, and out of the ecliptic from Ulysses allows us for the first time to form 2-point rough estimates of the instantaneous value of the A parameter, as follows. We use the inverse form of equation (2)

$$R_{sw}(\text{latitude}) = R_{sw}(\text{equator})*\left(1 - \text{A}\ \sin^2\ \text{latitude}\right) \qquad (4)$$

where R_{sw} is the H-H$^+$ charge exchange rate at 1 AU deduced from solar wind measurements. Measurements from two latitudes (1 and 2) then yield an estimate for A:

$$A = (R_1 - R_2)/\left(R_1 \sin^2(\text{latitude}_2) - \text{R}_2 \sin^2(\text{latitude}_1)\right) \qquad (5)$$

that is also plotted in Figure 3. This instantaneous estimate for A will not be meaningful in periods when Ulysses was near the ecliptic, so we have restricted the display to periods when Ulysses was poleward of 35 degrees N or S in heliographic latitude. The result is a bimodal set of points with large A near solar minimum and small A near solar maximum, the result we were expecting to find based on predictions by *Lallement et al.* [1985] and others. The technique has the obvious limitation of assuming that equation (4) and its assumed functional form are sufficiently close to the truth to be useful, which may not always be true. On the same plot we have shown some A values deduced from earlier remote sensing work for comparison.

[21] Figure 3 also shows updated A value estimates from the Ulysses GAS Lyman-α experiment. *Pryor et al.* [1998b] found A in the GAS data was small in the previous maximum and large in the last solar minimum. Our current modeling efforts use standard hot hydrogen density models and a detailed Lyman-α illumination model described by *Pryor et al.* [1996, 1998a, 1998b, 2001] that uses He 1083 nm solar images (spectroheliograms) processed into Carrington maps of He 1083 nm equivalent width by the National Solar Observatory to produce estimates of the solar Lyman-α flux for each day at each solar latitude and longitude. This technique has previously reproduced many details of the spatial and temporal variations in the Pioneer Venus, Galileo, and Ulysses Lyman-α data sets. The standard hot hydrogen density model also introduces north-south asymmetries because the upwind direction is out of the ecliptic plane at 5.2 ± 0.2 ecliptic latitude [*Witte et al.*, 2003]. Several important changes have been made since our earlier modeling efforts. The H atom temperature at large distances in the models is now 12000 K, not 8000 K, reflecting the recent work with SOHO SWAN absorption cell data by *Costa et al.* [1999]. Data are now included from directions more than 45 degrees from the Sun, relaxing our previous restriction to the anti-sunward hemisphere, based on additional study of the instrument scattering properties. We have also decided based on additional in-flight calibration work that the GAS background estimates described in *Pryor et al.* [1998b] were not adequate. We now use a least-

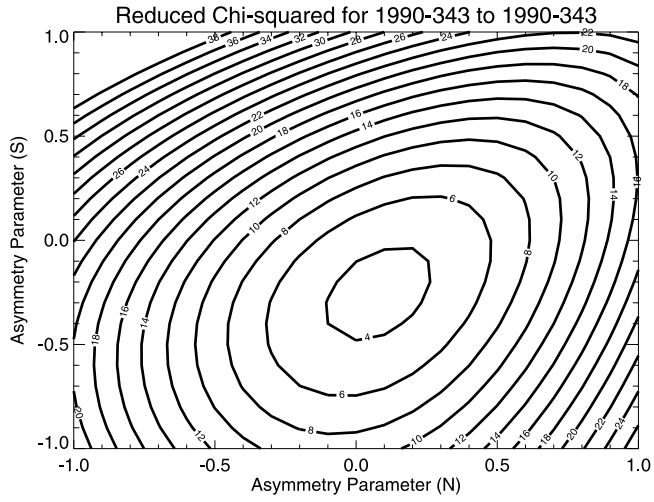

Figure 7. A contour plot of the reduced chi-squared fitting parameter for the GAS map from 1990-343 is shown. Twenty-one values of A_N and 21 values of A_S were tested, in the range from A = −1.0 to 1.0, providing 21 × 21 = 441 models for each map. In this case the minimum in reduced chi-square occurs for $A_N = 0.1$ and $A_S = -0.2$.

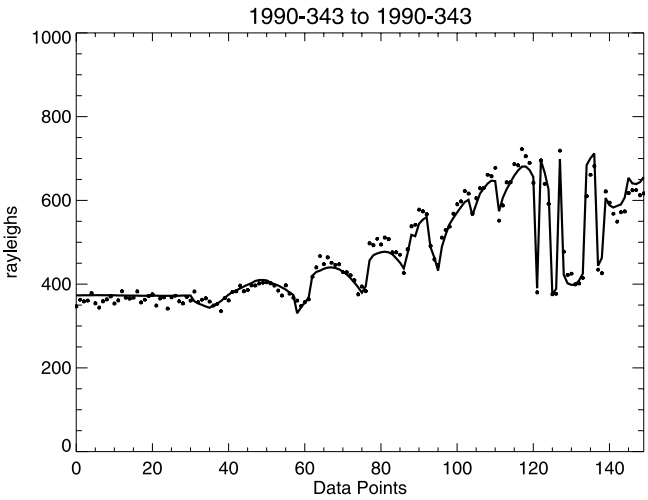

Figure 8. The same GAS map is shown in a point-by-point comparison with the best model found from Figure 9.

squares fit between the model and the data to estimate the background (Figure 6). We trust this technique because the model has been successful in fitting Galileo data where the background is well understood, since non-Lyman-α channels are available [*Pryor et al.*, 2001]. The solar wind asymmetry parameter in the north (A_N) and in the south (A_S) were varied separately. This additional degree of freedom proved very helpful in fitting real structure in the data. A grid search in A_N and A_S was performed (441 models per map) to choose A_N and A_S based on the model that minimized the reduced chi-square fitting parameter (Figure 7). Figure 8 shows the point-by-point agreement between data and model for the 1990 day 343 GAS map, and Figure 9 shows the distribution of data and model points in ecliptic latitude and longitude. Figure 10 is a color image of this data and model. O and B stars brighter than magnitude 6.0 were removed, forming an obvious arc across the map where the Milky Way falls. Figure 11 illustrates a sample retrieved asymmetry profile. We found that maps obtained well out of the plane of the ecliptic are still not well modeled and may be intrinsically unsuitable for finding A_N and A_S separately, since the two hemispheres both fall on the same lines-of-sight. Figure 3 only shows GAS asymmetry results obtained when Ulysses was within 30 degrees of the heliographic equator. Additional modeling effort will be required to understand the GAS maps obtained at higher latitudes. The GAS derived A values again show lower asymmetry during the previous solar maximum and higher asymmetry during the last solar minimum. The

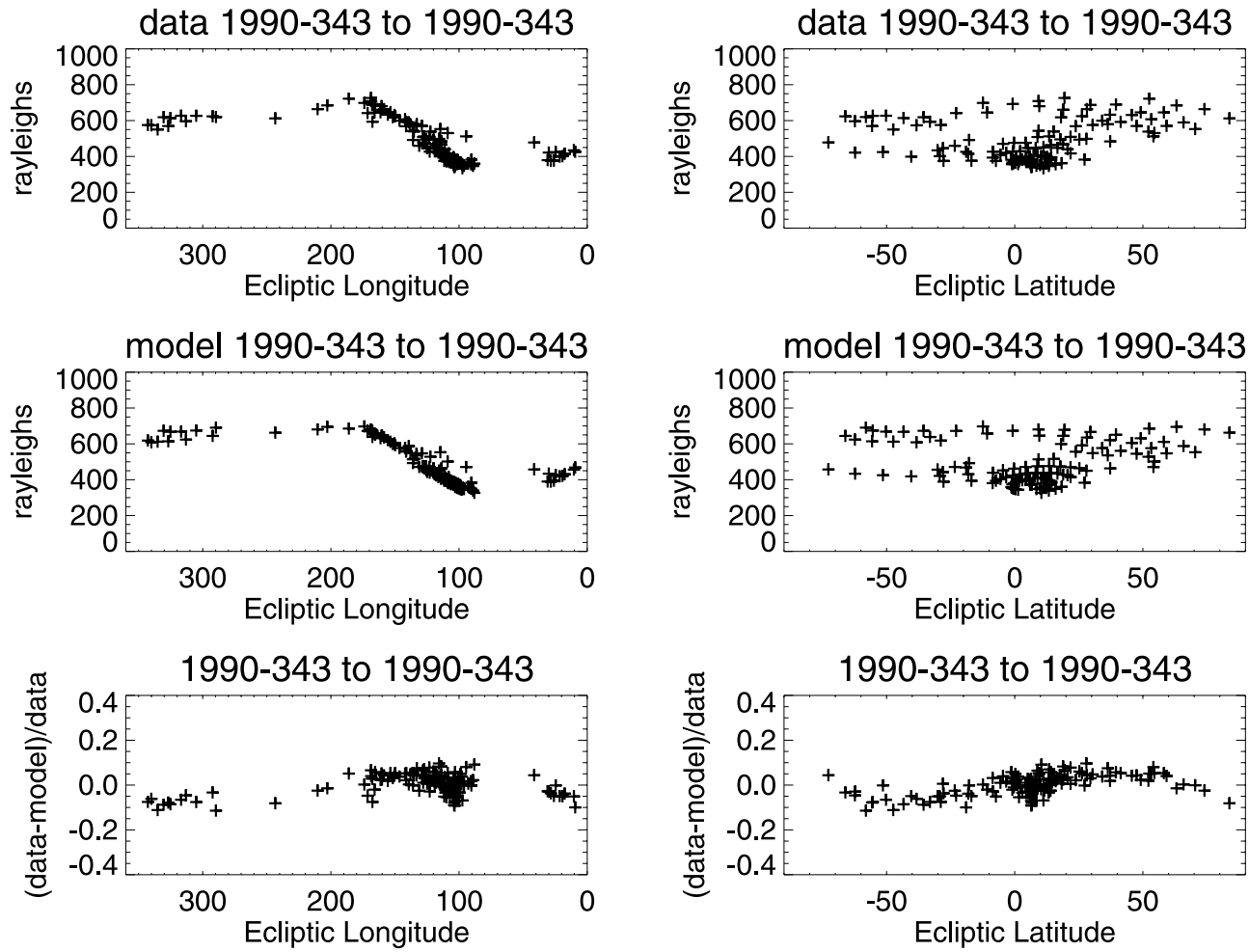

Figure 9. The same GAS map and model are shown point-by-point as a function of ecliptic latitude and longitude.

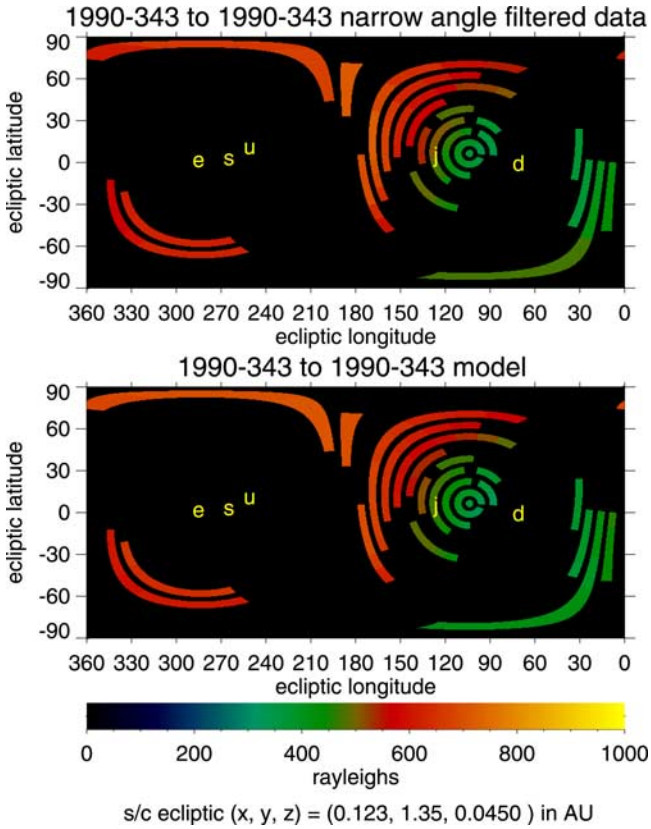

Figure 10. A color image shows the star-filtered GAS data as a function of ecliptic latitude and longitude and a model for this data. The positions of the Earth, Sun, Jupiter, upwind, and downwind are marked e, s, j, u, and d, respectively.

observing geometry during the current solar maximum was mostly unfavorable for the asymmetry determination, since Ulysses was mostly well out of the ecliptic.

5. Conclusions and Future Work

[22] The unique Ulysses out of the ecliptic solar wind measurements help to validate several decades of effort in the Lyman-α remote sensing field. The Ulysses SWOOPS solar wind data, both by themselves and in comparison with near-Earth satellite data, show that a more isotropic solar wind mass flux is present at solar maximum than at solar minimum. This is consistent with SOHO SWAN results which found an upwind heliospheric groove in 1996 near solar minimum, which gradually weakened and vanished as solar maximum approached and the heliospheric current sheet increased its inclination, spreading the more effective solar wind for charge exchange (dense and slow) over a wider range of latitudes.

[23] Comparison of Lyman-α data from various spacecraft beginning in 1974 shows that the general pattern found by the SOHO SWAN and Ulysses SWOOPS comparisons held in earlier epochs as well. When the heliospheric current sheet tilt was small during solar minimum, Prognoz, Mariner 10, Pioneer Venus, SWAN, and Ulysses GAS all found a Lyman-α brightness minimum in the upwind ecliptic direction, consistent with enhanced low-latitude charge exchange. When the heliospheric current sheet was more inclined closer to solar maximum, OGO-5, Galileo, Ulysses, and SWAN all found a brightness maximum in the upwind ecliptic direction, consistent with more latitudinally isotropic H-H^+ charge-exchange.

[24] The SWOOPS measurements have borne out the extensive earlier remote sensing work involving Lyman-α. Solar minimum provides extensive coronal holes at high latitudes that produce high-speed solar wind with reduced effectiveness in removing slow H. Low heliospheric current sheet tilt produces a low-latitude enhancement in the slow solar wind flux and carves a groove in the hydrogen distribution near the ecliptic plane. Solar maximum produces smaller coronal holes, a larger current sheet tilt that sprays slow, dense solar wind at a larger range of latitudes, and a resulting reduction in the H atom lifetime at high heliospheric latitudes, enlarging the polar cavity. Figure 3 of *McComas et al.* [1999] shows both the upwind heliospheric cavity shape from the solar minimum SWOOPS results, and the rounder shape found for a constant in latitude charge exchange rate, more appropriate for the solar maximum data presented here. Results on the solar wind proton mass flux distribution from earlier Lyman-α studies separated in time are now seen to be due to actual changes in the solar wind properties associated with changes in the current sheet tilt and the behavior of coronal holes over the solar cycle.

[25] A second remote sensing technique, studies of interplanetary scintillations, has also provided information on the latitude dependence of the mass flux [e.g., *Woo and Gazis*, 1994; *Woo and Goldstein*, 1994]. Woo found that the solar wind mass flux anisotropy was reduced at solar maximum. These results seem consistent with Lyman-α and solar wind results.

[26] One also expects the flux of pickup hydrogen ions produced by the H and H^+ charge-exchange process [*Vasyliunas and Siscoe*, 1976; *Gloeckler et al.*, 1993, 1994] to be more latitude-invariant at solar maximum based on the data in Figure 5. Detailed discussion of the variations in

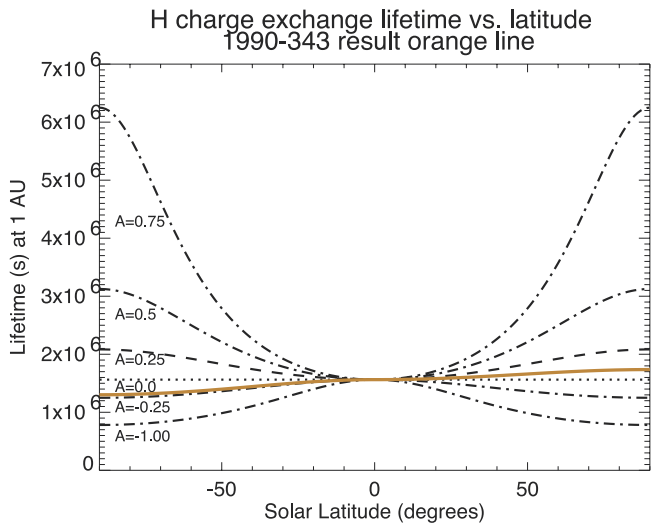

Figure 11. The retrieved $A_N = 0.1$ and $A_S = -0.2$ H atom lifetime against charge exchange profiles for the 1990-343 Ulysses GAS map are shown and compared with several other profiles.

latitude of the pickup ion flux over the solar cycle, including the effects of radiation pressure on the density distribution, is given by *Bzowski et al.* [2001b]. Their predictions could be tested using Ulysses SWICS (Solar Wind Ion Composition Spectrometer) data. Ulysses GAS and SWOOPS are expected to continue taking data for several more years, making it possible to study the reformation of the ecliptic heliospheric groove during the next solar minimum. We will look for a better parameterization of the anisotropies and their variations, as the traditional A parameter used here to illustrate the changes by comparisons between current data and literature values does not well represent the sharply defined heliospheric grooves seen at solar minimum [*Summanen et al.*, 1997; *Summanen*, 2000].

[27] **Acknowledgments.** We thank the European Space Agency (ESA) and NASA for supporting the Ulysses mission for many years. W. Pryor acknowledges support from the Office of Space Science Minority University Initiative at Hampton University. W. Pryor and J. Ajello acknowledge support from the NASA Ulysses (Heliospheric Missions) Guest Investigator Program. K. Tobiska and W. Pryor acknowledge support from NASA's Living With a Star Program. M. Witte acknowledges support from Deutsches Zentrum fur Luft- und Raumfahrt (DLR) under grant 50 0N 91035 for the Ulysses GAS experiment. D. McComas acknowledges support from the Ulysses Project for the SWOOPS experiment and from the ACE project for the SWEPAM experiment. We thank J. Harvey at the National Solar Observatory, T. Hoeksema, A. Lazarus, and K. Ogilvie for providing relevant data sets electronically.

[28] Shadia Rifai Habbal thanks Maciej Bzowski and Pradip Gangopadhyay for their assistance in evaluating this paper.

References

Ajello, J. M., An Interpretation of Mariner 10 helium (584 Å) and hydrogen (1216 Å) interplanetary emission observations, *Astrophys. J.*, *222*, 1068–1079, 1978.

Ajello, J. M., Solar minimum Lyman α sky background observations from Pioneer Venus Orbiter Ultraviolet Spectrometer: Solar wind latitude variation, *J. Geophys. Res.*, *95*, 14,855–14,861, 1990.

Ajello, J. M., N. Witt, and P. W. Blum, Four UV observations of the interstellar wind by Mariner 10: Analysis with spherically symmetric solar radiation models, *Astron. Astrophys.*, *73*, 260–271, 1979.

Ajello, J. M., W. R. Pryor, C. A. Barth, C. W. Hord, and K. E. Simmons, Solar wind latitude variations and multiple scattering from Galileo interplanetary Lyman-α observations, *Adv. Space Res.*, *13*, 37–40, 1993.

Ajello, J. M., W. R. Pryor, C. A. Barth, C. W. Hord, A. I. F. Stewart, K. E. Simmons, and D. T. Hall, Observations of interplanetary Lyman-α with the Galileo Ultraviolet Spectrometer: Multiple scattering effects at solar maximum, *Astron. Astrophys.*, *289*, 283–303, 1994.

Bame, S. J., D. J. McComas, B. L. Barraclough, J. L. Phillips, K. J. Sofaly, J. C. Chavez, B. E. Goldstein, and R. K. Sakurai, The Ulysses solar wind plasma experiment, *Astron. Astrophys. Suppl. Ser.*, *92*, 237–265, 1992.

Banks, P. M., and G. Kockarts, *Aeronomy*, part A, Academic, San Diego, Calif., 1973.

Barnett, C. F., Collisions of H, H_2, He, and Li atoms and ions with atoms and molecules, in *Atomic Data for Fusion*, *Tech. Rep. ORNL-6086*, vol. 1, Oak Ridge Natl. Lab., Oak Ridge, Tenn., 1990.

Bertaux, J. L., R. Lallement, V. G. Kurt, and E. N. Mironova, Characteristics of the local interstellar hydrogen determined from PROGNOZ 5 and 6 interplanetary Lyman-alpha line profile measurements with a hydrogen absorption cell, *Astron. Astrophys.*, *150*, 1–20, 1985.

Bertaux, J. L., et al., SWAN: A study of solar wind anisotropies on SOHO with Lyman Alpha sky mapping, *Sol. Phys.*, *162*, 403–439, 1995.

Bertaux, J. L., E. Quemerais, and R. Lallement, Observations of a groove in the interplanetary Lyman a sky pattern as a signature of enhanced ionization and solar wind mass flux in the neutral sheet, *Geophys. Res. Lett.*, *23*, 3675–3678, 1996.

Bertaux, J. L., E. Quemerais, R. Lallement, E. Kyrola, W. Schmidt, T. Summanen, J. P. Goutail, M. Berthe, J. Costa, and T. Holzer, First results from SWAN Lyman-α solar wind mapper on SOHO, *Sol. Phys.*, *175*, 737–770, 1997.

Bertaux, J. L., E. Kyrola, E. Quemerais, R. Lallement, W. Schmidt, T. Summanen, J. Costa, and T. Makinen, SWAN observations of the solar wind latitude distribution and its evolution since launch, *Space Sci. Rev.*, *87*, 129–132, 1999.

Broadfoot, A. L., and S. Kumar, The interstellar wind: Mariner 10 measurements of hydrogen (1216 Å) and helium (584 Å) interplanetary emission, *Astrophys. J.*, *222*, 1054–1067, 1978.

Bzowski, M., A model of charge exchange of interstellar hydrogen on a time-dependent, 2D solar wind, *Space Sci. Rev.*, *97*, 379–383, 2001a.

Bzowski, M., D. Rucinski, T. Summanen, and E. Kyrola, Expected fluxes of H+ pickup ions in the inner heliosphere during various phases of solar cycle, *Space Sci. Rev.*, *97*, 417–421, 2001b.

Bzowski, M., T. Summanen, D. Rucinski, and E. Kyrola, Response of interplanetary glow to global variations of hydrogen ionization rate and solar Lyman α flux, *J. Geophys. Res.*, *107*(A7), 1101, doi:10.1029/2001JA000141, 2002.

Costa, J., R. Lallement, E. Quemerais, J.-L. Bertaux, E. Kyrola, and W. Schmidt, Heliospheric interstellar H temperature from SOHO/SWAN H cell data, *Astron. Astrophys.*, *349*, 660–672, 1999.

Couzens, D. A., and J. H. King, Interplanetary medium data book, Suppl. 3, 1977–1985, *Rep. NSSDC-WDC-A-R&S 86-04*, NASA Goddard Space Flight Cent., Greenbelt, Md., 1986.

Gloeckler, G., J. Geiss, H. Balsiger, L. A. Fisk, A. B. Galvin, F. M. Ipavich, K. W. Ogilvie, R. von Steiger, and B. Wilken, Detection of interstellar pick-up hydrogen in the solar system, *Science*, *261*, 70–73, 1993.

Gloeckler, G., J. R. Jokipii, J. Giacalone, and J. Geiss, Concentration of interstellar pickup H(+) and He(+) in the solar wind, *Geophys. Res. Lett.*, *21*, 1565–1568, 1994.

Gruntman, M. A., New channel for the photoionization of hydrogen atoms in the solar system, in *Physics of the Outer Heliosphere*, *COSPAR Colloquium Ser.*, vol. 1, edited by S. Grzedzielski and D. E. Page, pp. 83–86, Pergamon, New York, 1990.

Hoeksema, J. T., Large-scale solar and heliospheric magnetic fields, *Adv. Space Res.*, *11*, 15–24, 1991.

Hoeksema, J. T., J. M. Wilcox, and P. H. Scherrer, Structure of the heliospheric current sheet in the early portion of sunspot cycle 21, *J. Geophys. Res.*, *87*, 10,331–10,338, 1982.

Hoeksema, J. T., J. M. Wilcox, and P. H. Scherrer, The structure of the heliospheric current sheet: 1978–1982, *J. Geophys. Res.*, *88*, 9910–9918, 1983.

Hord, C. W., W. E. McClintock, A. I. F. Stewart, C. A. Barth, L. W. Esposito, G. E. Thomas, B. R. Sandel, D. M. Hunten, A. L. Broadfoot, and D. E. Shemansky, The Galileo Ultraviolet Spectrometer Experiment, *Space Sci. Rev.*, *60*, 503–530, 1992.

Izmodenov, V. V., J. Geiss, R. Lallement, G. Gloeckler, V. B. Baranov, and Y. G. Malama, Filtration of interstellar hydrogen in the two-shock heliospheric interface: Inferences on the local interstellar cloud electron density, *J. Geophys. Res.*, *104*, 4731–4741, 1999.

King, J. H., Interplanetary medium data book, *Rep. NSSDC/WDC-A-R&S 77-04*, NASA Goddard Space Flight Cent., Greenbelt, Md., 1977.

King, J. H., Interplanetary medium data book, Suppl. 1, 1975–1978, *Rep. NSSDC/WDC-A-R&S 79-08*, NASA Goddard Space Flight Cent., Greenbelt, Md., 1979.

King, J. H., Interplanetary medium data book, Suppl. 4, 1985–1988, *Rep. NSSDC-WDC-A-R&S 89-17*, NASA Goddard Space Flight Cent., Greenbelt, Md., 1989.

King, J. H., and N. E. Papitashvili, Interplanetary medium data book, Suppl. 5, 1988–1993, *Rep. NSSDC/WDC-A-R&S 94-08*, NASA Goddard Space Flight Cent., Greenbelt, Md., 1994.

Kumar, S., and A. L. Broadfoot, Evidence from Mariner 10 of Solar Wind Flux Depletion at High Ecliptic Latitudes, *Astron. Astrophys.*, *69*, L5–L8, 1978.

Kumar, S., and A. L. Broadfoot, Signatures of solar wind latitudinal structure in interplanetary Lyman-α emissions: Mariner 10 observations, *Astrophys. J.*, *228*, 302–311, 1979.

Kyrola, E., T. Summanen, T. Makinen, E. Quemerais, J.-L. Bertaux, R. Lallement, and J. Costa, Preliminary retrieval of solar wind latitude distribution from Solar Wind Anisotropies/SOHO observations, *J. Geophys. Res.*, *103*, 14,523–14,538, 1998.

Lallement, R., and A. I. Stewart, Out-of-ecliptic Lyman-α observations with Pioneer Venus: Solar wind anisotropy degree in 1986, *Astron. Astrophys.*, *227*, 600, 1990.

Lallement, R., J. L. Bertaux, and V. G. Kurt, Solar wind decrease at high heliographic latitudes detected from Prognoz interplanetary Lyman Alpha mapping, *J. Geophys. Res.*, *90*, 1413–1423, 1985.

Lallement, R., J. L. Bertaux, E. Chassefiere, and B. R. Sandel, Lyman-alpha observations from Voyager (1–18 AU), in *Physics of the Outer Heliosphere*, *COSPAR Colloquium Ser.*, vol. 1, edited by S. Grzedzielski and D. E. Page, pp. 73–82, Pergamon, New York, 1990.

McComas, D. J., The three-dimensional structure of the solar wind over the solar cycle, paper presented at Solar Wind 10, Inst. of Interplanet. Space Phys., Pisa, Italy, 16–21 June 2002.

McComas, D. J., S. J. Bame, P. Barker, W. C. Feldman, J. L. Phillips, P. Riley, and J. W. Griffee, Solar Wind Electron Proton Alpha Monitor

(SWEPAM) for the Advanced Composition Explorer, *Space Sci. Rev.*, *86*, 563–612, 1998.

McComas, D. J., H. O. Funsten, J. T. Gosling, and W. R. Pryor, Ulysses measurements of variations in the solar wind-interstellar hydrogen charge exchange rate, *Geophys. Res. Lett.*, *26*, 2701–2704, 1999.

McComas, D. J., B. L. Barraclough, H. O. Funsten, J. T. Gosling, E. Santiago-Munoz, R. M. Skoug, B. E. Goldstein, M. Neugebauer, P. Riley, and A. Balogh, Solar wind observations over Ulysses' first full polar orbit, *J. Geophys. Res.*, *105*, 10,419–10,434, 2000a.

McComas, D. J., J. T. Gosling, and R. Skoug, Ulysses observations of the irregularly structured mid-latitude solar wind during the approach to solar maximum, *Geophys. Res. Lett.*, *27*, 2437–2440, 2000b.

McComas, D. J., R. Goldstein, J. T. Gosling, and R. M. Skoug, Ulysses' second orbit: Remarkably different solar wind, in *The 3-D Heliosphere at Solar Maximum*, edited by R. G. Marsden, pp. 393–399, Kluwer Acad., Norwell, Mass., 2001.

McComas, D. J., H. A. Elliot, and R. von Steiger, Solar wind from high latitude coronal holes at solar maximum, *Geophys. Res. Lett.*, *29*(9), 1314, doi:10.1029/2001GL013940, 2002a.

McComas, D. J., H. A. Elliot, J. T. Gosling, D. B. Reisenfeld, R. M. Skoug, B. E. Goldstein, M. Neugebauer, and A. Balogh, Ulysses' second fast-latitude scan: Complexity near solar maximum and the reformation of polar coronal holes, *Geophys. Res. Lett.*, *29*(9), 1290, doi:10.1029/2001GL014164, 2002b.

Ogawa, H. S., C. Y. R. Wu, P. Gangopadhyay, and D. L. Judge, Solar photoionization as a loss mechanism of neutral interstellar hydrogen in interplanetary space, *J. Geophys. Res.*, *100*, 3455–3462, 1995.

Ogilvie, K., et al., SWE: A comprehensive plasma instrument for the WIND spacecraft, *Space Sci. Rev.*, *71*, 55–77, 1995.

Pryor, W. R., J. M. Ajello, C. A. Barth, C. W. Hord, A. I. F. Stewart, K. E. Simmons, W. E. McClintock, B. R. Sandel, and D. E. Shemansky, The Galileo and Pioneer Venus ultraviolet spectrometer experiments—Solar Lyman-alpha latitude variation at solar maximum from interplanetary Lyman-alpha observations, *Astrophys. J.*, *394*, 363–377, 1992.

Pryor, W. R., et al., Latitude variations in interplanetary Lyman alpha data from the Galileo EUVS modeled with solar He 1083 nm images, *Geophys. Res. Lett.*, *23*, 1893–1896, 1996.

Pryor, W. R., S. J. Lasica, A. I. F. Stewart, D. T. Hall, S. Lineaweaver, W. B. Colwell, J. M. Ajello, O. R. White, and W. K. Tobiska, Interplanetary Lyman alpha observations from Pioneer Venus over a solar cycle from 1978 to 1992, *J. Geophys. Res.*, *103*, 26,833, 1998a.

Pryor, W. R., M. Witte, and J. M. Ajello, Interplanetary Lyman-α remote sensing with the Ulysses Interstellar Neutral Gas Experiment, *J. Geophys. Res.*, *103*, 26,813–26,832, 1998b.

Pryor, W. R., I. Stewart, K. Simmons, M. Witte, J. Ajello, K. Tobiska, D. J. McComas, and D. Hall, Remote sensing of H from Ulysses and Galileo, in *The 3-D Heliosphere at Solar Maximum*, edited by R. G. Marsden, pp. 393–399, Kluwer Acad., Norwell, Mass., 2001.

Rucinski, D., et al., Ionization processes in the heliosphere-rates and methods of their determination, *Space Sci. Rev.*, *103*, 26,813, 1996.

Stewart, A. I. F., Design and operation of the Pioneer Venus Orbiter ultraviolet spectrometer, *IEEE Trans. Geosci. Remote Sens.*, *18*, 165, 1980.

Summanen, T., The solar ionization rate of the interplanetary hydrogen as a function of a heliomagnetic latitude: A new model for the interplanetary Lyman alpha studies, *Astrophys. Space Sci.*, *274*, 143–148, 2000.

Summanen, T., R. Lallement, and E. Quemerais, Solar wind proton flux latitude variations: Comparison between Ulysses in situ data and indirect measurements from interstellar Lyman-α mapping, *J. Geophys. Res.*, *102*, 7051–7062, 1997.

Summanen, T., J. T. T. Makinen, E. Kyrola, W. Schmidt, T. I. Pulkinnen, J.-L. Bertaux, R. Lallement, and E. Quemerais, Interplanetary Lyman alpha observations of SWAN during the rising phase of the 23rd solar cycle, *Adv. Space Res.*, *29*, 457–462, 2002.

Thomas, G. E., The interstellar wind and its influence on the interplanetary environment, *Annu. Rev. Earth Planet Sci.*, *6*, 173–204, 1978.

Thomas, G. E., and R. F. Krassa, OGO 5 measurements of the Lyman Alpha sky background, *Astron. Astrophys.*, *11*, 218–233, 1971.

Tobiska, W. K., T. Woods, F. Eparvier, R. Viereck, L. Floyd, D. Bouwer, G. Rottman, and O. R. White, The SOLAR2000 empirical solar irradiance model and forecast tool, *J. Atmos. Sol. Terr. Phys.*, *62*, 1233–1250, 2000.

Vasyliunas, V. M., and G. L. Siscoe, On the flux and the energy spectrum of interstellar ions in the solar system, *J. Geophys. Res.*, *81*, 1247–1252, 1976.

Witt, N., P. W. Blum, and J. M. Ajello, Solar wind latitudinal variations deduced from Mariner 10 interplanetary H (1216 Å) observations, *Astron. Astrophys.*, *73*, 272–281, 1979.

Witt, N., J. M. Ajello, and P. W. Blum, Polar solar wind and interstellar wind properties from interplanetary Lyman-α radiation measurements, *Astron. Astrophys.*, *95*, 80–85, 1981.

Witte, M., H. Rosenbauer, E. Keppler, H. Fahr, P. Hemmerich, H. Lauche, A. Loidl, and R. Zwick, The interstellar neutral-gas experiment on Ulysses, *Astron. Astrophys. Suppl. Ser.*, *92*, 333–348, 1992.

Witte, M., M. Banaszkiewicz, and H. Rosenbauer, Recent results on the parameters of the interstellar helium from the Ulysses/Gas Experiment, *Space Sci. Rev.*, *78*, 289–296, 1996.

Witte, M., M. Banszkiewicz, H. Rosenbauer, and D. McMullin, Kinetic parameters of interstellar helium: Updated results from the Ulysses/GAS instrument, *Adv. Space Res*, in press, 2003.

Woo, R., and P. R. Gazis, Mass flux in the ecliptic plane and near the Sun deduced from Doppler scintillations, *Geophys. Res. Lett.*, *21*, 1101–1104, 1994.

Woo, R., and R. M. Goldstein, Latitudinal variation of speed and mass flux in the acceleration region of the solar wind inferred from spectral broadening measurements, *Geophys. Res. Lett.*, *21*, 85–88, 1994.

J. M. Ajello, Jet Propulsion Laboratory, M. S. 183-601, 4800 Oak Grove Drive, Pasadena, CA 91109, USA. (jajello@mail1.jpl.nasa.gov)

D. J. McComas, Space Science and Engineering Division, Southwest Research Institute, 6220 Culebra Road, San Antonio, TX 78238, USA. (dmccomas@swri.edu)

W. R. Pryor, Center for Atmospheric Sciences, Hampton University, 23 Tyler Street, Hampton, VA 23668, USA. (wayne.pryor@hamptonu.edu)

W. K. Tobiska, Space Environment Technologies SpaceWx Division, 1676 Palisades Drive, Pacific Palisades, CA 90272, USA. (ktobiska@spaceenvironment.net)

M. Witte, Max-Planck Institut fur Aeronomie, Max-planck-Str. 2, Katlenburg-Lindau, 47191, Germany. (witte@linmpi.mpg.de)